


Fractional Order Intelligent Robust Controller for a Flexible Link Robot Manipulator: Real-Time Experimental Implementation

Fatemeh Abbasi, Hadi Delavari*

Department of Electrical Engineering, Hamedan University of Technology, Hamedan, Iran

ARTICLE INFO

Article Type

Original Research

Article History

Received: August 27, 2025

Revised: October 19, 2025

Accepted: November 03, 2025

ePublished: November 21, 2025

ABSTRACT

The study introduces an effective control approach designed for a flexible single-link robotic manipulator, offering advantages such as operational capability in harsh environments, ease of component movement, and lower manufacturing and maintenance costs compared to rigid manipulators. Despite these advantages, controlling such systems remains challenging due to their nonlinear dynamics and the unwanted vibrations caused by link flexibility, which can significantly affect positioning accuracy and stability. To address these challenges, the proposed fractional-order fuzzy sliding mode controller (FO-FSMC) integrates the robustness and stability features of sliding mode control with the adaptability and decision-making capability of fuzzy logic, while also exploiting the precision and memory characteristics offered by fractional calculus. The performance and effectiveness of the proposed control strategy are verified through practical real-time implementation on a single-link flexible robotic manipulator. The results show that the proposed FO-FSMC under different inputs exhibits superior tracking accuracy and faster convergence compared to the classical PID controller. Compared with the conventional SMC, the FO-FSMC achieved slightly higher accuracy and smoother control signals for sinusoidal and mixed inputs, while it showed significant improvement for pulse and step inputs with lower IAE and RMSE, minimum tracking error, and faster adaptation. These results establish FO-FSMC as a robust and practical candidate for real-time control of flexible manipulators, making it well-suited for diverse industrial and research applications.

Keywords: Single Link Flexible Robot Manipulator, Sliding Mode Control, Fuzzy Control, Fractional Calculus, PID Control, Experimental Results, Uncertainties

How to cite this article

Abbasi F, Delavari H, Fractional order intelligent robust controller for a flexible link robot manipulator: Real-time experimental implementation. *Modares Mechanical Engineering*; 2025;25(11):703-715.

*Corresponding author's email: delavari@hut.ac.ir

*Corresponding ORCID ID: 0000-0002-5718-933X



Copyright© 2025, TMU Press. This open-access article is published under the terms of the Creative Commons Attribution-NonCommercial 4.0 International License which permits Share (copy and redistribute the material in any medium or format) and Adapt (remix, transform, and build upon the material) under the Attribution-NonCommercial terms.

1- Introduction

In recent years, flexible robotic manipulators have garnered significant attention in various industries, including manufacturing, aerospace [1], biomedical engineering [2], and micro robotics, due to their advantages, such as low weight, reduced energy consumption, high response speed, and the ability to interact with delicate objects. Using a lightweight and flexible structure, these manipulators enhance operational efficiency. For instance, in applications that require precise physical interaction with fragile objects, structural flexibility prevents excessive forces that could damage the object. However, these advantages present significant control challenges. Structural flexibility results in phenomena such as deflection and vibration in the robot links, complicating accurate position control. These vibrations directly affect tracking accuracy and increase system error. Therefore, designing a robust controller capable of accurately and rapidly tracking a reference trajectory is paramount. Various control strategies, including classical PID, sliding mode control (SMC), adaptive SMC, fuzzy logic-based controllers, and fractional-order control methods, have been investigated to address these challenges. Previous studies have applied classical PID control to single flexible-link manipulators [3], demonstrating satisfactory trajectory control in simulation. However, these works were limited to simulated environments and did not address the challenges of real-time implementation, vibration uncertainties, or chattering reduction. In contrast, the present study develops a fractional-order fuzzy sliding mode controller (FO-FSMC), experimentally implemented on a real flexible-link manipulator. The proposed approach leverages the robustness of sliding mode control, while the fuzzy logic component smooths the control signal, significantly reducing chattering. Additionally, the fractional-order sliding surface improves transient response and adaptability, enabling precise trajectory tracking under practical operating conditions. These enhancements collectively demonstrate a clear advantage over conventional PID approaches, both in terms of robustness and real-time applicability.

Unlike previous works [4] that used conventional or adaptive SMC under ideal modeling assumptions, this study presents an experimental FO-FSMC that combines the robustness of SMC, the smooth control of fuzzy logic, and the flexibility of fractional calculus to reduce chattering and enhance tracking performance. Experimental results on a real setup confirm its superior effectiveness compared to traditional SMC and PD controllers.

Previous works such as the Fuzzy-FOPID control of a rigid two-link manipulator optimized via metaheuristic algorithms [5] and GA-based adaptive PID controllers [6] were validated only through simulation, whereas the present FO-FSMC approach is experimentally implemented on a flexible-link manipulator, demonstrating enhanced robustness, reduced chattering, and superior trajectory tracking performance.

Although some studies have experimentally implemented fractional-order or fuzzy PID controllers on flexible-link manipulators [7], these approaches remain limited in addressing strong nonlinearities and ensuring robustness theoretically. In the present work, FO-FSMC integrates fractional calculus, fuzzy logic, and sliding mode control to suppress vibrations, reduce chattering, and theoretically guarantee robustness through Lyapunov-based stability analysis, while being experimentally validated on a real flexible-link manipulator.

Other studies that combined ADRC and sliding mode techniques [8], fractional-order sliding mode controllers optimized via PSO [9], and fractional-order sliding mode control (FOSMC) [10] have primarily relied on numerical simulations. The proposed FO-FSMC extends these concepts by providing experimental validation on a real flexible-link setup and integrating fuzzy inference within the fractional-order sliding surface to enable smoother control action and reduced chattering, which were not addressed in earlier works.

Similar approaches employing fractional-order controllers combined with sliding mode and intelligent PID strategies [11,12,13,14,15] have

been reported, but these works either focused on rigid manipulators or lacked experimental verification. The present FO-FSMC method further integrates fuzzy logic inference into the fractional-order sliding surface, experimentally validating its effectiveness in vibration suppression, chattering reduction, and robust trajectory tracking.

Additional studies that applied fuzzy sliding mode controllers (FSMC) [16,17] to single-link manipulators showed improved robustness and reduced control effort in simulations. However, these works did not experimentally validate the proposed methods. In contrast, FO-FSMC is implemented on a real flexible-link manipulator, combining fractional-order dynamics with fuzzy sliding surfaces to achieve smoother control, further reduction of chattering, and robust trajectory tracking under real-time conditions.

Article [18] demonstrates that flexible-link manipulators exhibit nonlinear dynamics and may show instability and chaotic behavior. Using Hamilton's principle with nonlinear strain assumptions, the dynamic equations are derived and analyzed through bifurcation diagrams, Poincare maps, and Lyapunov exponents. Experimental results indicate that low input amplitudes produce subharmonic or quasi-periodic responses, while higher amplitudes lead to quasi-periodic/chaotic behavior without damaging the joints. In [19] models friction in mechanical arms as the difference between input and output angles, estimating its parameters using direct and recursive least-squares identification methods. The identified friction model enables effective SDRE-based nonlinear optimal control for a two-DOF mechanical arm. Experimental validation on a single arm shows that compensating friction with the proposed controller significantly reduces the end-effector tracking error.

Collectively, these comparisons highlight that although various combinations of fractional calculus, fuzzy logic, and sliding mode control have been proposed, existing studies are often limited to simulations, or rigid manipulator setups. The novelty of the present work lies in the experimental implementation of a hybrid FO-FSMC on a real flexible-link manipulator, which simultaneously addresses chattering reduction, vibration suppression, precise trajectory tracking, and robustness against model uncertainties, with theoretical guarantees provided through Lyapunov-based stability analysis.

In summary, the main advantages and contributions of this work are as follows:

- Reduction of chattering and improvement of tracking accuracy by introducing fuzzy logic and fractional calculus in the controller design.
- Maintaining high performance and optimal behavior despite the use of estimated system dynamic parameters, ensuring robustness against model uncertainties.
- Robust stability analysis is theoretically proved, providing theoretical guarantees for its effectiveness under various operating conditions.
- Experimental implementation of the proposed method under real conditions verified the proposed technique performance

These contributions and advantages collectively demonstrate that the proposed approach not only mitigates the drawbacks of conventional methods but also achieves superior tracking performance with proven stability.

2- Robot dynamic model

A schematic of a single-link flexible mechanical arm is shown in Figure 1. This mechanical arm consists of a flexible arm of length l and an endpoint mass m . The variable θ is the angular position of the hub (rigid body), and δ is the displacement observed at the tip of the flexible structure.

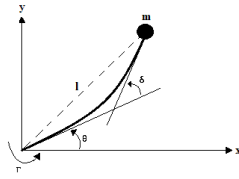


Figure 1. schematic of a single-link flexible arm

In this section, the dynamic model of a robot with n flexible arms is introduced. An easy way to estimate the dynamics of a flexible robot is to use the Mode-shape method. Assuming the Euler-Bernoulli beam model, the elastic beam deflection $w_i(\eta, t)$ of the i th link is expressed as a sum of infinite terms:

$$w_i(\eta, t) = \sum_{j=1}^{\infty} q_{ij}(t) \varphi_{ij}(\eta) \quad (1)$$

where $q_{ij}(t)$ is the time-varying amplitude of the mode j of the i th link and $\varphi_{ij}(\eta)$ is the mode-shift function that describes the displacement of the mode j of the i th link deflection. η also represents the displacement of the i th link in each axis direction.

Considering the flexibility of the link, a solution for the motion of the i th link is obtained using the short-constrained approximation. The solution obtained for the i th link is in the form of the following equation:

$$w_i(\eta, t) = \sum_{j=1}^{m_i} q_{ij}(t) \varphi_{ij}(\eta) \quad (2)$$

where m_i is the number of modes used to describe the deviation of the i th link.

Using the Euler-Bernoulli method, the following model is obtained [7,9].

$$M(\theta, \delta) \begin{bmatrix} \ddot{\theta} \\ \ddot{\delta} \end{bmatrix} + \begin{bmatrix} C_1(\dot{\theta}, \dot{\delta}) \\ C_2(\dot{\theta}, \dot{\delta}) \end{bmatrix} + \begin{bmatrix} G_1(\theta, \delta) \\ G_2(\theta, \delta) \end{bmatrix} + \begin{bmatrix} 0 & 0 \\ 0 & K \end{bmatrix} \begin{bmatrix} \theta \\ \delta \end{bmatrix} = \begin{bmatrix} u \\ 0 \end{bmatrix} \quad (3)$$

Where:

δ denotes the displacement observed at the tip of the flexible structure, u is the applied torque, $C_1(\dot{\theta}, \dot{\delta})$, $C_2(\dot{\theta}, \dot{\delta})$ include the Coriolis and centrifugal forces, $G_1(\theta, \delta)$, $G_2(\theta, \delta)$ represent the influence of gravity on the structure, θ refers to the ball unit's angular position, $M(\theta, \delta)$ is the inertia matrix obtained from the mass and geometric parameters of the links, and K is the stiffness matrix related to the material properties and flexibility of the links.

Matrix multiplication in equation 1 yields two equations:

The dynamic of a flexible link may be considered as an n -degree-of-freedom system and partitioned as vectors $\delta \in R^l$, $\theta \in R^m$, and $u \in R^m$. Accordingly, by definition of $\hat{G}_1(\theta, \dot{\theta}, \delta, \dot{\delta}) = C_1(\dot{\theta}, \dot{\delta}) + G_1(\theta, \delta)$ and $\hat{G}_2(\theta, \dot{\theta}, \delta, \dot{\delta}) = C_2(\dot{\theta}, \dot{\delta}) + G_2(\theta, \delta)$, the dynamic of an n -degree-of-freedom system can be written as:

$$M_{11}\ddot{\theta} + M_{12}\ddot{\delta} + \hat{G}_1 = u \quad (4)$$

$$M_{21}\ddot{\theta} + M_{22}\ddot{\delta} + \hat{G}_2 + K\delta = 0 \quad (5)$$

From equation 5, we have:

$$\ddot{\delta} = -M_{22}^{-1}(M_{21}\ddot{\theta} + \hat{G}_2 + K\delta) \quad (6)$$

Then, by substituting 6 into 4, we have:

$$\bar{M}\ddot{\theta} + \bar{K} + \bar{G} = u \quad (7)$$

$$\bar{M} = M_{11} - M_{12}M_{22}^{-1}M_{21} \quad (8)$$

$$\bar{G} = \hat{G}_1 - M_{12}M_{22}^{-1}\hat{G}_2 \quad (9)$$

$$\bar{K} = -M_{12}M_{22}^{-1}K\delta \quad (10)$$

The final form of the system's dynamic model, derived from equation 5, is presented as follows:

$$\ddot{\theta} = -\bar{M}^{-1}(\bar{K} + \bar{G}) + \bar{M}^{-1}u \quad (11)$$

From Equation 11, we can obtain estimates of \hat{f} and \hat{b} given $\ddot{\theta} = f + bu$:

$$\hat{f} = -\bar{M}^{-1}(\bar{K} + \bar{G}) \quad (12)$$

$$\hat{b} = \bar{M}^{-1} \quad (13)$$

In this article, the matrix M is assumed to have dimensions 3×3 [12]. (Note that the dimensions of other matrices and vectors will also change relative to the matrix M .)

$$M = \begin{bmatrix} 3.6892 \times 10^{-4} & -9.9976 \times 10^{-5} & -9.9976 \times 10^{-5} \\ -9.9976 \times 10^{-5} & 0.0216 & 0 \\ -9.9976 \times 10^{-5} & 0 & 0.0216 \end{bmatrix}, \quad K = \begin{bmatrix} 0 & 0 & 0 \\ 0 & 83 & 0 \\ 0 & 0 & 879 \end{bmatrix}, \quad G = \begin{bmatrix} 0 \\ 0 \\ 0 \end{bmatrix}$$

In this study, the Euler-Bernoulli beam theory is adopted to model the flexible link for the following reasons. First, the link under consideration is slender and lightweight (length 30 cm, thickness 2 mm, weight 100–200 g), giving a high length-to-thickness ratio ($L/h = 150$). Its material (Plexiglas) and light structure make shear deformation and rotary inertia negligible compared to bending deformations. Under these conditions, the Euler-Bernoulli model accurately captures the dominant vibration modes without unnecessary complexity.

Second, this formulation provides a clear representation of the link's vibrational behavior, which is the main focus of this work. Using this model, the primary vibration modes can be efficiently analyzed, while the resulting dynamic equations remain simple and computationally tractable. These characteristics justify the adoption of the Euler-Bernoulli beam theory in modeling the flexible link [20].

3- experimental setup

In the practical implementation of the flexible-link robot, the essential components include a motor and a motor-to-computer interface. The flexible link is a Plexiglas beam with a thickness of 2 mm, a length of 30 cm, and a weight of approximately 100–200 g. Its high flexibility allows the vibrations and oscillations to be clearly observable. The motor used is a Dynamixel AX-18A, providing the minimum torque required to actuate the link.

The motor includes embedded sensors such as speed, position, torque, load, and temperature, which can be used for real-time feedback. The motor specifications and setup instructions are provided in [21–23]. For real-time communication, a USB2Dynamixel interface with a baud rate of 100,000 was employed, enabling fast and reliable transmission of tip position or angular position data. The motor is powered by a 12 V, 2.5 A DC supply, and its drivers can be installed via RoboPlus, allowing straightforward interfacing with the computer. This experimental setup provides a practical basis for implementing the control strategies described in the following sections. It allows the measured data to be captured in real time and fed into MATLAB/Simulink for control signal computation. The setup ensures that the system behavior can be accurately monitored and controlled before presenting the results of the proposed FO-FSMC controller.

The various components of the experimental setup can be seen in Figure 2.

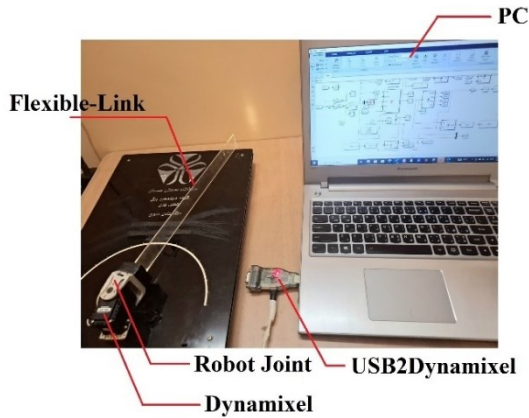


Figure 2. Single-link flexible robot manipulator

4- Controller design

4-1 Fractional calculus

Fractional calculus is a generalization of integer-order ordinary differential equations that can provide more accurate models of dynamical systems that have properties such as self-similarity and memory of system states. This unique capability offers improved accuracy in describing real-world dynamical systems, particularly those with complex or nonlinear behaviors. Fractional calculus operators enable controllers to precisely tune the system dynamics over a wider frequency range, which is not comparable to that of conventional integer-order controllers. In control systems, the use of fractional calculus has gained popularity due to the improvement of system performance, such as increased robustness, reduced overshoot, and smoother responses.

The application of the gamma function marks an initial step in fractional-order calculus. This function, which is a generalization of the factorial concept for real and complex numbers, is one of the special and important functions in fractional-order mathematics. This function is represented as follows:

$$\Gamma(z) = \int_0^{\infty} e^{-t} t^{z-1} dt \quad (14)$$

The Caputo fractional derivative, often used in fractional-order dynamic equations, can be formulated using the gamma function, as given in Equation 15.

$${}_a^C D_t^p f(t) = \frac{1}{\Gamma(n-p)} \int_a^t (t-\tau)^{n-p-1} f^{(n)}(\tau) d\tau, \quad n-1 < p < n \quad (15)$$

It is important to note that various definitions of the fractional-order derivative have been proposed. However, since the initial conditions for the derivatives of Caputo-type fractional differential equations are similar to those of integer-order differential equations, this definition is more applicable than other definitions. Therefore, in fractional-order differential equations, the Caputo derivative is commonly employed.

4-2 Sliding mode control

Sliding Mode Control (SMC) is a nonlinear control technique known for its robustness, accuracy, and ease of implementation. It operates by driving the system states toward a predefined manifold in the state space, referred to as the sliding surface, and then maintaining them on it. This control method involves two key steps: first, designing a sliding surface that satisfies the design specifications for the desired sliding motion; and second, formulating a control law to ensure the system trajectories reach and remain on this surface. One of the key advantages of SMC is that a properly selected sliding surface allows engineers to enforce specific system behaviors. Additionally, once the system is in sliding mode, its response becomes largely insensitive to model uncertainties, external disturbances, and nonlinearities. This makes SMC particularly effective for controlling complex nonlinear systems under uncertain conditions.

In general, the sliding surface is defined according to Equation 16.

$$S = \left(\frac{d}{dt} + \lambda \right)^{n-1} e \quad (16)$$

Where, λ is a positive coefficient and n indicates the order of the system.

We define the sliding surface in this article as follows:

$$S = k_1 e + k_2 \dot{e} + k_3 D^{\alpha} e \quad (17)$$

Tracking error is expressed as:

$$e = x - x_d \quad (18)$$

By differentiating Equation 17 and setting it equal to $-k \cdot \text{sign}(S)$, the total control law is obtained as follows:

$$\dot{S} = k_1 \dot{e} + k_2 \ddot{e} + k_3 D^{\alpha+1} e = -k \text{sign}(S) \quad (19)$$

$$u = \frac{1}{k_2 b} (-k \text{sign}(S) - k_1 \dot{e} - k_2 \ddot{e} + k_2 \ddot{x}_d - k_3 D^{\alpha+1} e) \quad (20)$$

4-3 Fuzzy control

The signum function used in equations 19 and 20 is known to cause chattering in the control signal. To reduce this effect, a fuzzy controller replaces the signum function in the control law of Equation 20. This integration of fuzzy logic with sliding mode control (SMC) combines the strengths of both methods, resulting in a controller with both robustness and adaptability. The fuzzy sliding mode controller operates based on the following table of IF-THEN rules:

Table 1. Rule base for K_F

S / \dot{S}	P	Z	N
P	NH	NS	PM
Z	NB	ZE	PB
N	NM	PS	PH

A sample rule can be interpreted from the table as follows:

If $S = P$ and $\dot{S} = P$ then $K_F = NH$

In this fuzzy rule base, the symbols NH, NB, NM, NS, ZE, PS, PM, PB, and PH refer to the linguistic values: negative huge, negative big, negative medium, negative small, zero, positive small, positive medium, positive big, and positive huge, respectively. The fuzzy membership functions corresponding to these linguistic terms are triangular and must be carefully designed to ensure effective control performance. Their structure is shown in Figure 3 [24,25].

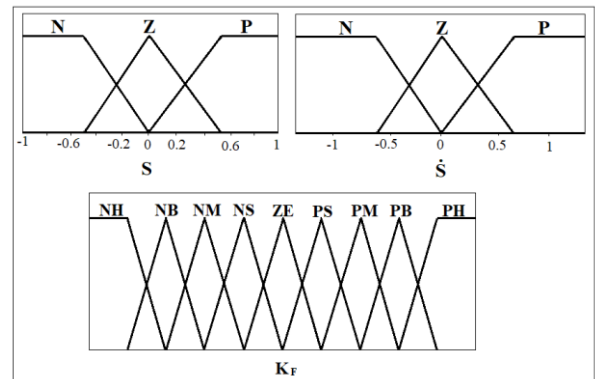


Figure 3. Triangle membership functions, fuzzification, and defuzzification

5- Stability analysis

Here, the stability of the closed-loop system under the control signal obtained in the controller design section is analyzed [26]. First, the following Lyapunov function candidate is constructed:

$$V = \frac{1}{2} S^2 \quad (21)$$

The estimation error can be defined as follows:

$$|f - \hat{f}| \leq F, \quad G_{min} < |\hat{b}b^{-1}| \leq G_{max} \quad (22)$$

By taking the derivative with respect to t , we have:

$$\dot{V} = S\dot{S} = S(k_1 \dot{e} + k_2 \ddot{e} + k_3 D^{\alpha+1} e) = S(k_1 \dot{e} + k_2 (\ddot{x} - \ddot{x}_d) + k_3 D^{\alpha+1} e) = S(k_1 \dot{e} + k_2 (f + bu - \ddot{x}_d) + k_3 D^{\alpha+1} e) \leq \eta |S| \quad (23)$$

By substituting equation 20 into equation 23, we have:

$$\begin{aligned} \dot{V} = & S \left(k_1 \dot{e} + k_2 \left(f + b \left(\frac{1}{k_2 b} (-k \operatorname{sign}(S) - k_1 \dot{e} - k_2 \hat{f} + k_2 \ddot{x}_d - \right. \right. \right. \\ & \left. \left. \left. k_3 D^{\alpha+1} e \right) - \ddot{x}_d \right) + k_3 D^{\alpha+1} e \right) = S (k_1 \dot{e} + k_2 f - \\ & b \hat{b}^{-1} k \operatorname{sign}(S) - b \hat{b}^{-1} k_1 \dot{e} - b \hat{b}^{-1} k_2 \hat{f} + b \hat{b}^{-1} k_2 \ddot{x}_d - \\ & b \hat{b}^{-1} k_3 D^{\alpha+1} e - k_2 \ddot{x}_d + k_3 D^{\alpha+1} e) = S (k_2 f - b \hat{b}^{-1} k \operatorname{sign}(S) + \\ & (1 - b \hat{b}^{-1})(k_1 \dot{e} - k_2 \ddot{x}_d + k_3 D^{\alpha+1} e) - b \hat{b}^{-1} k_2 \hat{f}) \leq \eta |S| \end{aligned} \quad (24)$$

By multiplying both sides of equation 24 by the expression $b^{-1} \hat{b}$ and adding the expression $b^{-1} \hat{b} k_2 \hat{f}$ and subtracting it on the left side of the inequality, we have:

$$\begin{aligned} \dot{V} = & S (b^{-1} \hat{b} k_2 f - k \operatorname{sign}(S) + (b^{-1} \hat{b} - 1)(k_1 \dot{e} - k_2 \ddot{x}_d + \\ & k_3 D^{\alpha+1} e) + b^{-1} \hat{b} k_2 \hat{f} - b^{-1} \hat{b} k_2 \hat{f} - k_2 \hat{f}) = S (b^{-1} \hat{b} k_2 (f - \hat{f}) - \\ & k \operatorname{sign}(S) + (b^{-1} \hat{b} - 1)(k_1 \dot{e} - k_2 \ddot{x}_d + k_3 D^{\alpha+1} e + k_2 \hat{f})) \leq \\ & -b^{-1} \hat{b} \eta |S| \end{aligned} \quad (25)$$

According to inequalities 25 and 22, we can write:

$$\begin{aligned} |S| |b^{-1} \hat{b} k_2 f| - k |S| + |S| |b^{-1} \hat{b} - 1| |k_1 \dot{e} - k_2 \ddot{x}_d + k_3 D^{\alpha+1} e| \leq \\ -b^{-1} \hat{b} \eta |S| \end{aligned} \quad (26)$$

Finally, the robust stability condition can be derived as inequality 27:

$$k \geq b^{-1} \hat{b} k_2 f + b^{-1} \hat{b} \eta + |b^{-1} \hat{b} - 1| |k_1 \dot{e} - k_2 \ddot{x}_d + k_3 D^{\alpha+1} e| \quad (27)$$

As a result, if the gain of the switching control law is as follows, the nonlinear system under sliding mode control with the control law 20, despite the uncertainty in the functions f and b will be stable.

$$k \geq G_{\max} (k_2 f + \eta) + |G_{\max} - 1| |k_1 \dot{e} - k_2 \ddot{x}_d + k_3 D^{\alpha+1} e| \quad (28)$$

6- Experimental implementation results

In this section, the proposed fractional-order fuzzy sliding mode controller (FO-FSMC) is practically implemented on a single-link flexible robotic manipulator to evaluate its effectiveness in real-time operation. To assess its performance against a widely adopted control approach, several different types of reference signals are used for testing and comparison. The experimental implementation results under these scenarios demonstrate that the FO_FSMC significantly outperforms other controller in tracking the reference signals.

6-1 Scenario I

To further validate the effectiveness of the proposed FO-FSMC controller, its performance was evaluated under a step reference input (at $t=1$ s, for an angle change from 30° to 150°) and compared with both the conventional PID and standard SMC controllers. The step input is commonly used to assess the transient behavior and steady-state accuracy of control systems. As shown in Figures 4-9, all controllers were able to track the desired reference trajectory; however, the proposed FO-FSMC exhibited faster convergence and smoother transient response. The controller achieves effective results by combining the robust performance of sliding mode control, the adaptable qualities of fuzzy logic, and the unique memory properties provided by fractional-order calculus. In this structure, the fuzzy logic adaptively generates the discontinuous control term $k \cdot \operatorname{sign}(s)$ in real time, based on the current system state, enabling the controller to handle nonlinearities and sudden changes intelligently. Simultaneously, due to the memory-retaining property and hereditary characteristics inherent in fractional calculus, the controller achieves improved and smoother performance. As a result, the FO-FSMC achieves a fast-settling time, low transient error, and high tracking accuracy. In contrast, the classical PID controller, due to its simple structure and fixed parameters, fails to adapt to the system's nonlinear and time-varying behavior, leading to slower response and higher tracking errors.

Although the performance of the FO-FSMC and SMC controllers appears close in terms of transient characteristics, the quantitative comparison in Table 2 highlights the superior accuracy and robustness of the proposed method. Specifically, the FO-FSMC achieved lower Integral of Absolute Error (IAE) and Root Mean Square Error (RMSE) values compared to both PID and SMC controllers. This demonstrates the controller's improved ability to suppress residual vibrations and reduce chattering effects while maintaining high tracking precision.

Table 2. Comparison of the performance of the methods in scenario I

	FO-FSMC	SMC	PID
IAE	3.438	4.257	7.834
RMSE	10.91	12.42	16.68

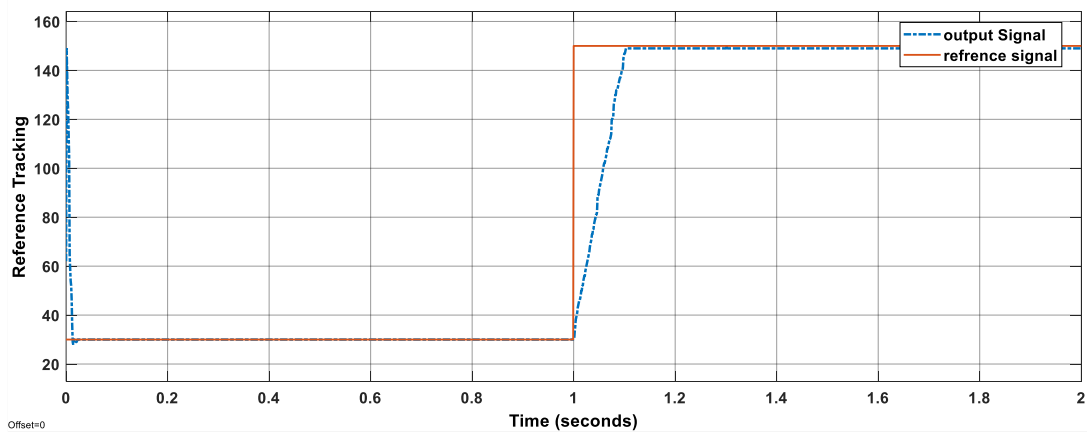


Figure 4. Step input tracking using the PID controller

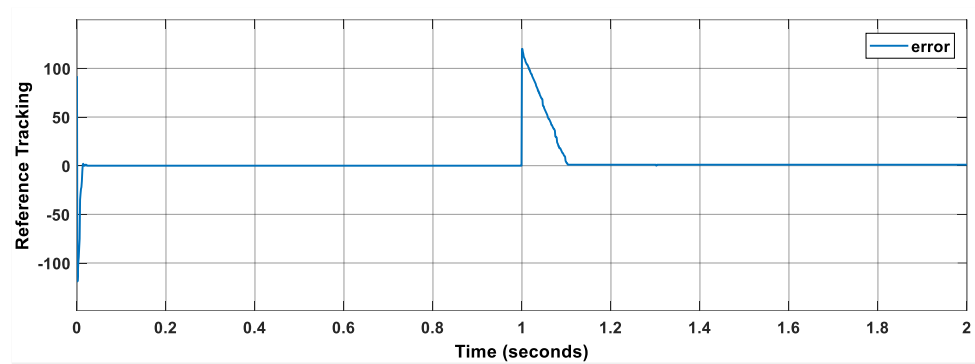


Figure 5. Step input tracking error using the PID controller

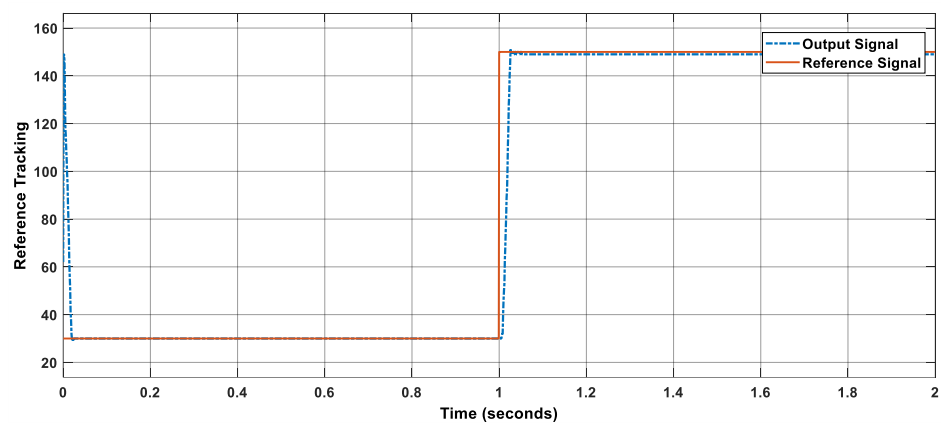


Figure 6. Step input tracking using the SMC controller

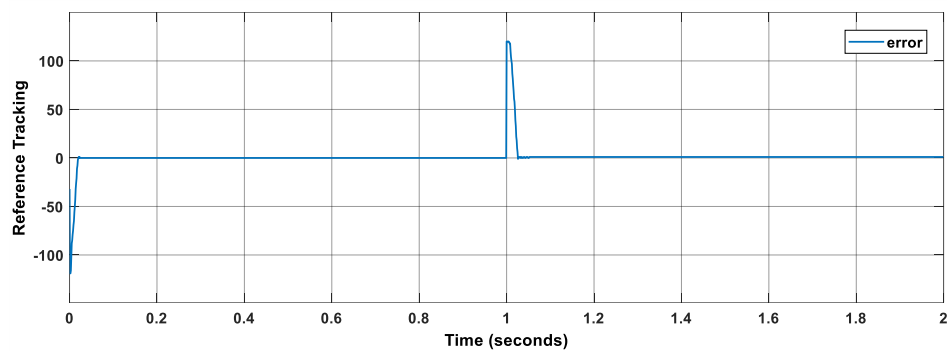


Figure 7. Step input tracking error using the SMC controller

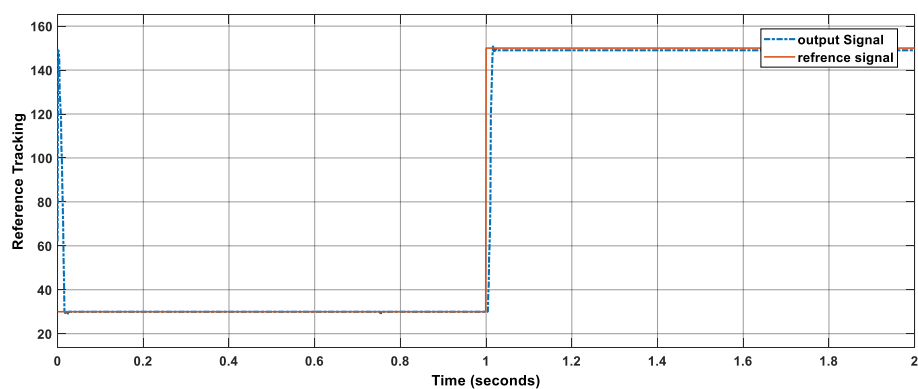


Figure 8. Step input tracking using the FO-FSMC controller

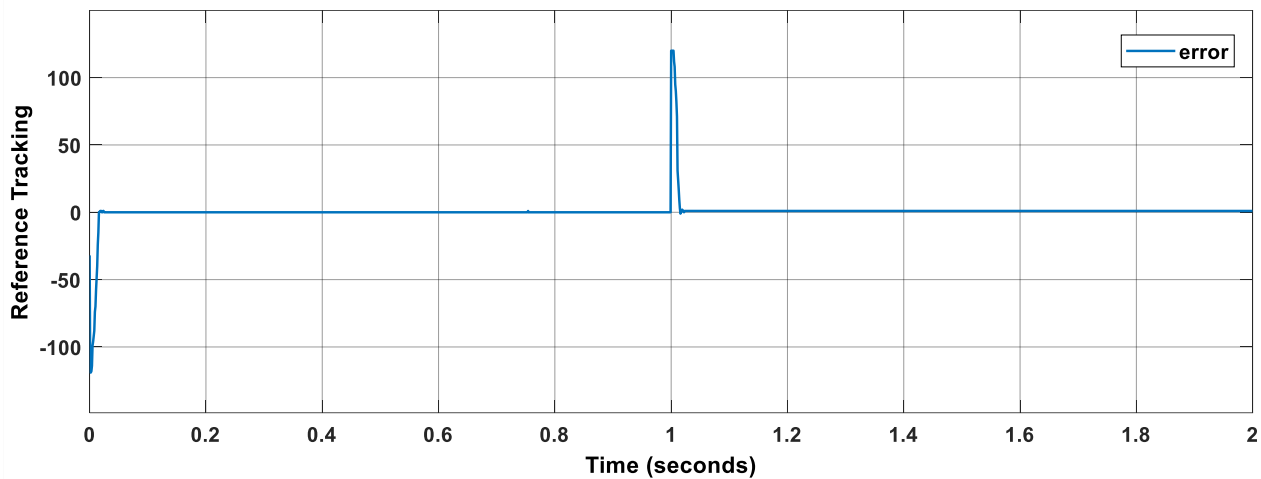


Figure 9. Step input tracking error using the FO-FSMC controller

6-2 Scenario II

To further evaluate the dynamic performance of the proposed controller, a sinusoidal reference trajectory ($r(t) = 60 \sin(4\pi t) + 90$) was applied to the flexible-link manipulator. This test aims to assess the controller's capability to handle continuous and smooth variations in the desired position, which closely represent practical operating conditions.

As illustrated in Figures 10-15, The PID controller, constrained by its fixed gains, cannot cope with the time-varying dynamics of the sinusoidal reference. Consequently, higher tracking errors occur, particularly around $t=1$ s. while both the conventional SMC and the proposed FO-FSMC successfully track the sinusoidal reference with minimal steady-state error. The performance of the two methods appears quite similar in this case, as the fractional-order and fuzzy components primarily enhance smoothness and adaptability during transient changes. The tracking responses of both controllers are

nearly indistinguishable in the sinusoidal test, confirming that the proposed fractional-order fuzzy design does not compromise the nominal performance of the conventional SMC while maintaining stable operation.

Quantitatively, the RMSE and IAE indices in Table 3 for the FO-FSMC are slightly lower than SMC, indicating comparable overall performance with improved somewhat smoothness. These results confirm that, even under periodic reference conditions, the proposed controller maintains precise trajectory tracking and stable vibration suppression without compromising robustness.

Table 3. Comparison of the performance of the methods in scenario II

	FO-FSMC	SMC	PID
IAE	1.534	1.585	1.955
RMSE	2.286	3.086	3.983

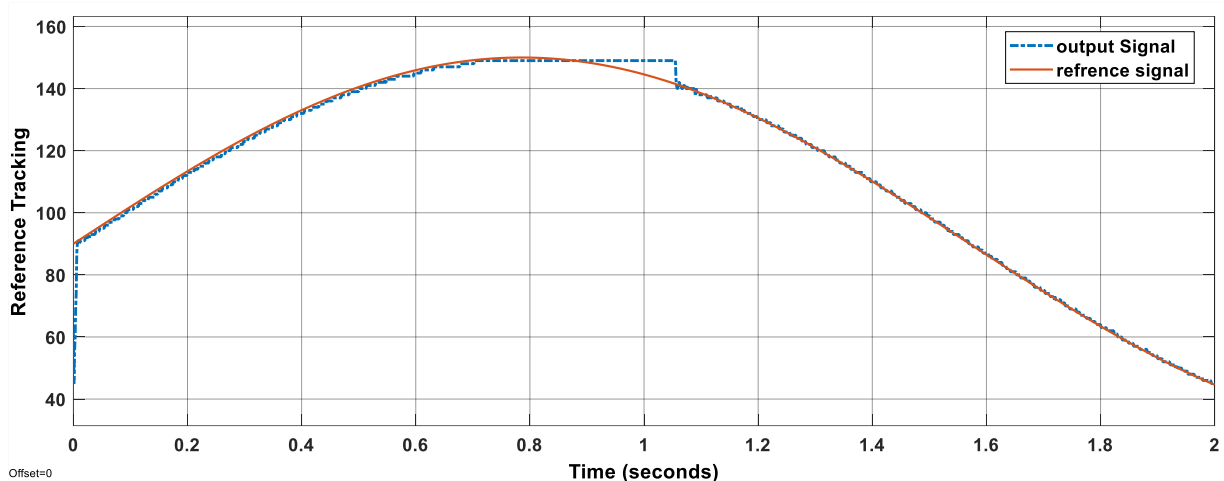


Figure 10. Sinusoidal input tracking using the PID controller

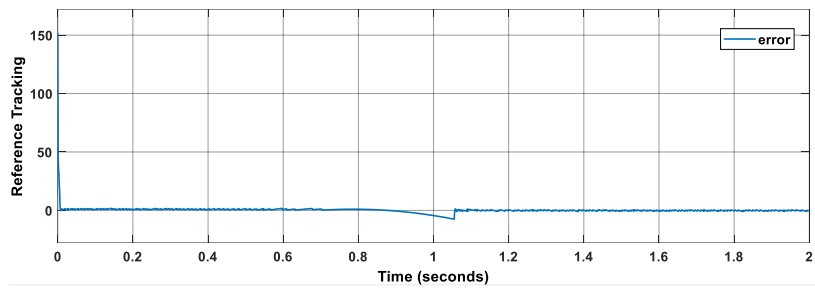


Figure 11. Sinusoidal input tracking error using the PID controller

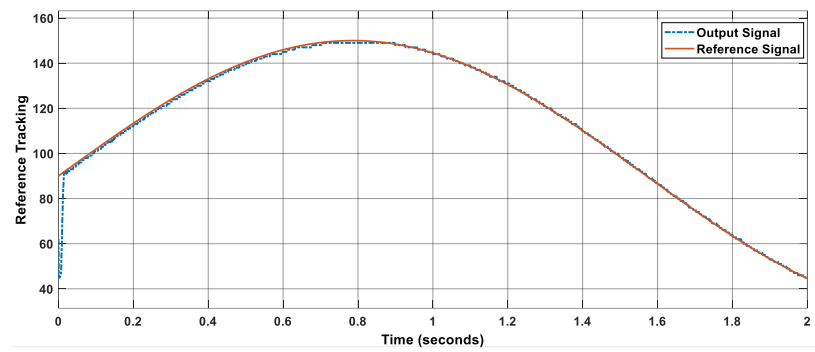


Figure 12. Sinusoidal input tracking using the SMC controller

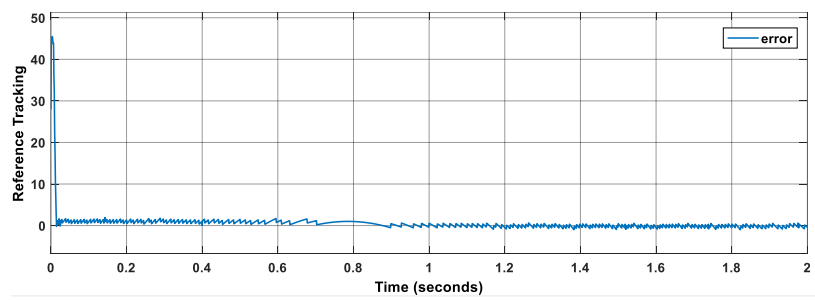


Figure 13. Sinusoidal input tracking error using the SMC controller

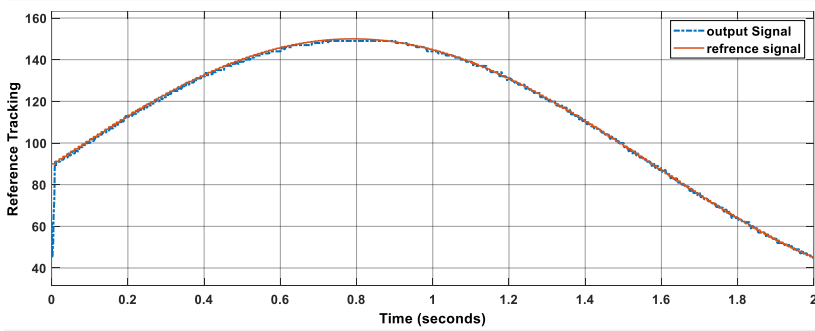


Figure 14. Sinusoidal input tracking using the FO-FSMC controller

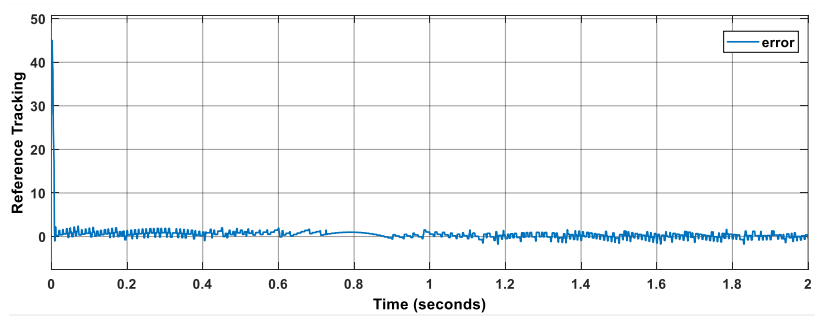


Figure 15. Sinusoidal input tracking error using the FO-FSMC controller

6-3 Scenario III

To further evaluate the robustness and transient response of the proposed controller, a pulse reference trajectory was applied to the flexible-link manipulator. This test is particularly suitable for assessing the controller's ability to handle abrupt reference changes and dynamic uncertainties.

As shown in Figures 16-21, the PID controller exhibits a relatively large tracking error and slow response to the sudden reference change, primarily due to its limited robustness against nonlinear dynamics and structural flexibility. The conventional SMC improves the response significantly by reducing tracking error; however, noticeable chattering still appears in the control signal. In contrast, the proposed FO-FSMC demonstrates superior performance in this case. It achieves a faster convergence to the desired trajectory with smaller steady-state error compared to both PID and SMC. The fuzzy inference

mechanism effectively smooths the control action, while the fractional-order sliding surface enhances adaptability to rapid transients. Quantitative results based on RMSE and IAE indices in Table 4 confirm that the FO-FSMC outperforms both PID and SMC, providing higher tracking accuracy and smoother control effort. These findings clearly demonstrate the advantage of integrating fractional calculus and fuzzy logic within the sliding mode control framework, especially under non-smooth reference conditions.

Table 4. Comparison of the performance of the methods in scenario III

	FO-FSMC	SMC	PID
IAE	6.58	9.32	18.32
RMSE	16.05	19.77	27.13

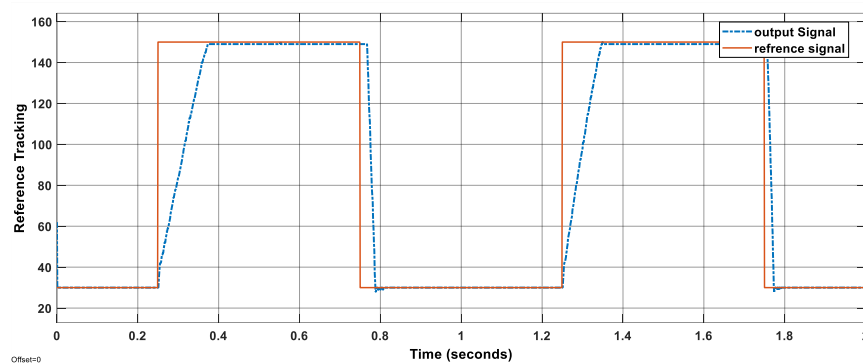


Figure 16. pulse input tracking using the PID controller

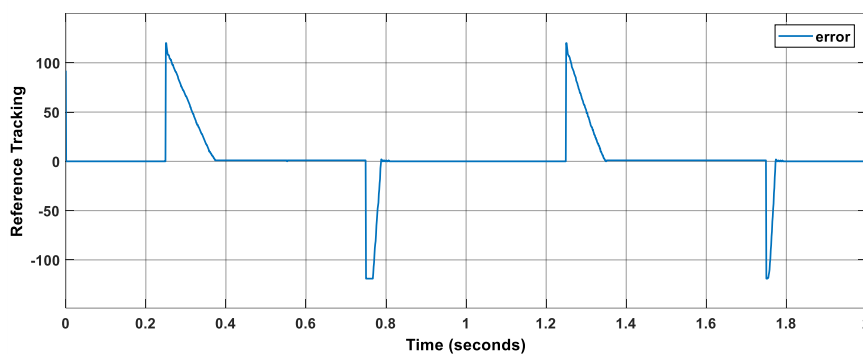


Figure 17. pulse input tracking error using the PID controller

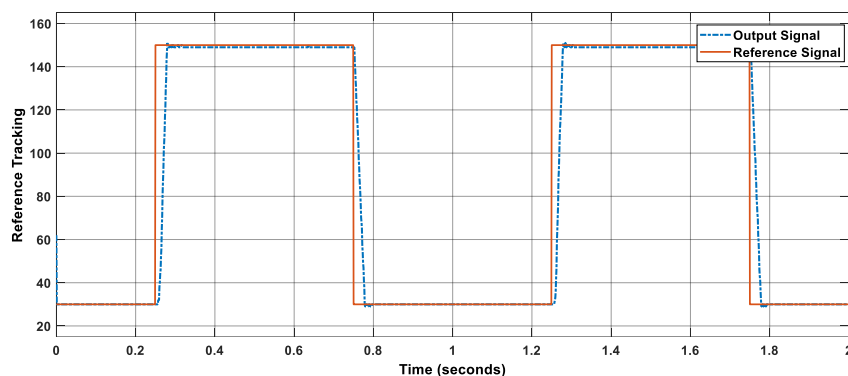


Figure 18. pulse input tracking using the SMC controller

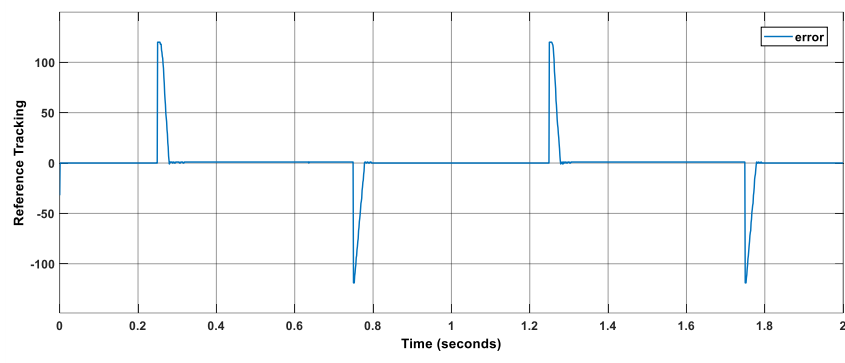


Figure 19. pulse input tracking error using the SMC controller

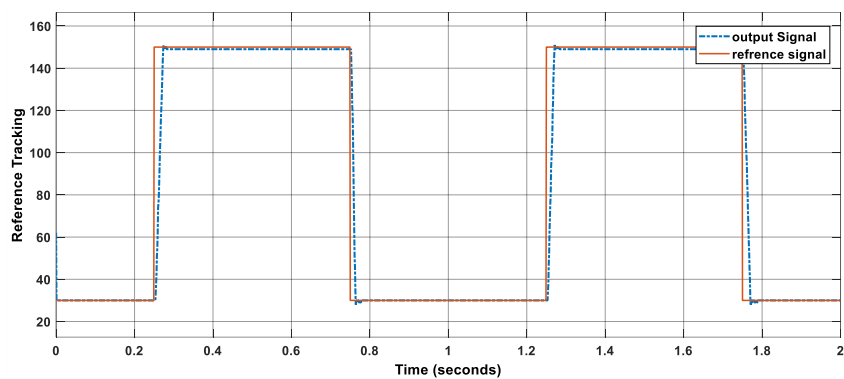


Figure 20. pulse input tracking using the FO-FSMC controller

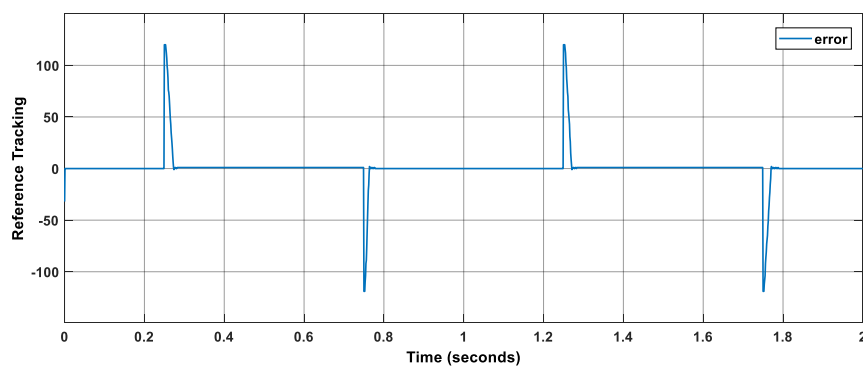


Figure 21. pulse input tracking error using the FO-FSMC controller

6-4 Scenario IV

To further evaluate the controller's performance under mixed and abrupt reference variations, a hybrid input was applied to the flexible-link manipulator. The reference trajectory initially follows a sinusoidal signal ($r(t) = 60 \sin(4\pi t) + 90$), to which a step input with a final value of 50° is added at $t = 1.5$ s. This test effectively examines the controller's capability to handle both periodic and sudden changes in the desired trajectory.

As illustrated in Figures 22-27, the PID controller shows a noticeable tracking error and slower adjustment after the step occurs, due to its limited robustness against nonlinear dynamics and abrupt reference changes. Both the conventional SMC and the proposed FO-FSMC achieve significantly better tracking accuracy and faster adaptation. In this scenario, the responses of FO-FSMC and SMC are approximately similar, both providing fast and accurate trajectory tracking with

minimal overshoot and small steady-state error. However, the proposed FO-FSMC achieves slightly higher tracking precision, owing to the fuzzy logic inference and fractional-order sliding surface. Quantitative comparisons based on RMSE and IAE indices in Table 5 confirm that both SMC-based methods outperform the PID controller, while the FO-FSMC provides marginal improvement in smoothness and overall control efficiency.

Table 5. Comparison of the performance of the methods in scenario IV

	FO-FSMC	SMC	PID
IAE	1.396	1.436	2.159
RMSE	2.336	2.455	4.561

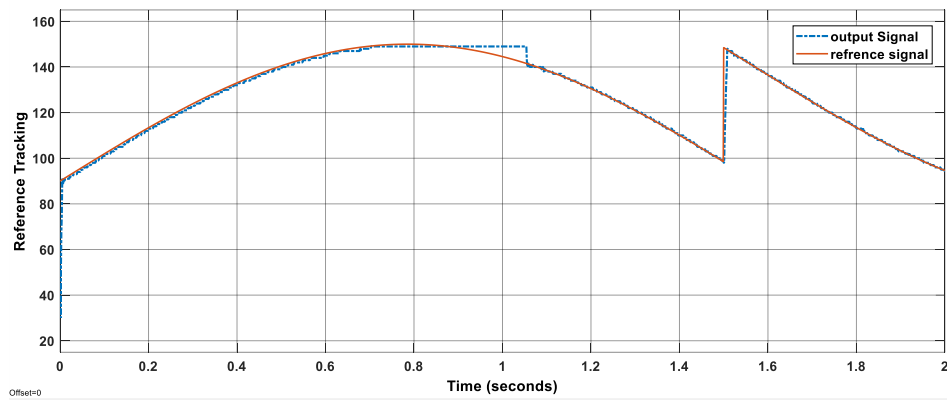


Figure 22. Hybrid input tracking using the PID controller

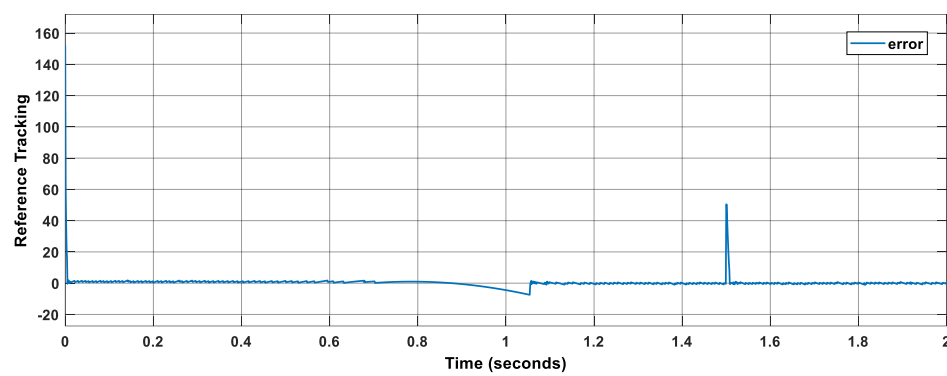


Figure 23. Hybrid input tracking error using the PID controller

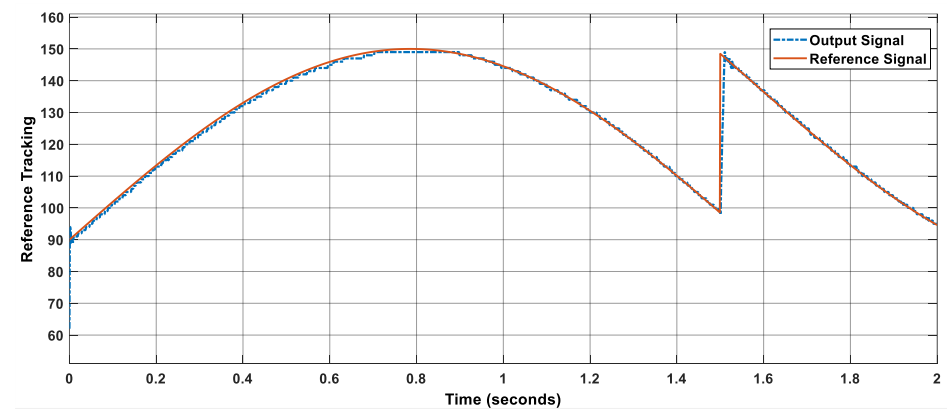


Figure 24. Hybrid input tracking using the SMC controller

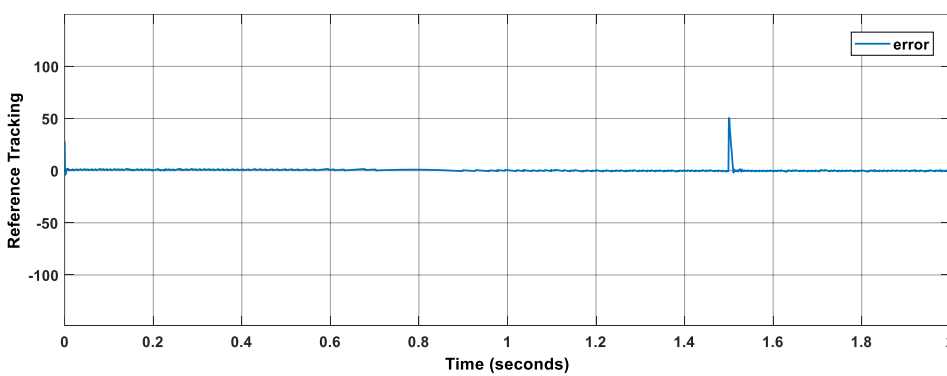


Figure 25. Hybrid input tracking error using the SMC controller

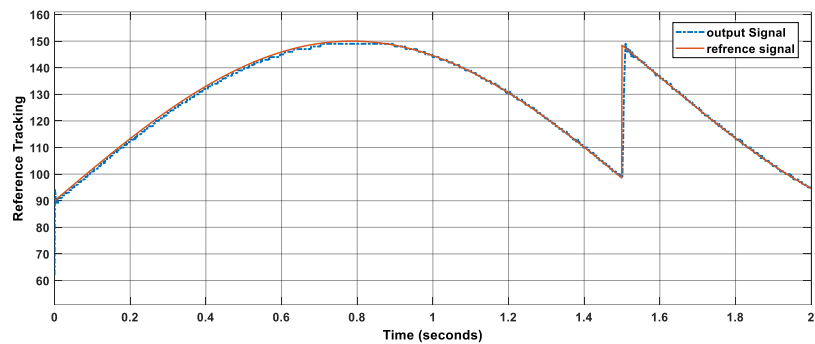


Figure 26. Hybrid input tracking using the FO-FSMC controller

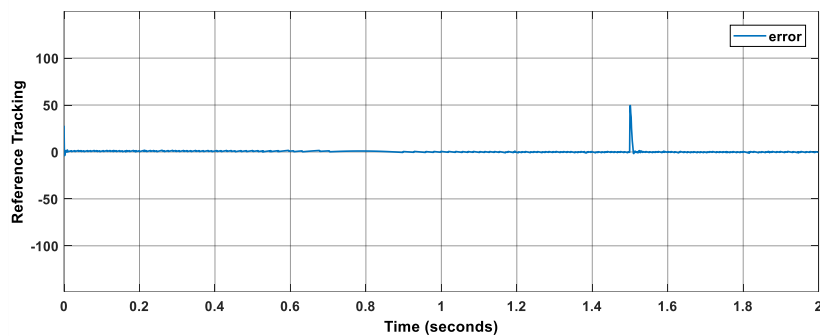


Figure 27. Hybrid input tracking error using the FO-FSMC controller

7- Conclusion

This study proposed a fractional-order fuzzy sliding mode controller (FO-FSMC) for a single-link flexible robotic manipulator, integrating the adaptive nature of fuzzy logic with the robustness of sliding mode control and the memory-enhancing characteristics of fractional calculus.

The controller was evaluated under four types of reference inputs: step, sinusoidal, pulse, and combined sinusoidal-step. For the step input, the FO-FSMC achieves the lowest IAE (3.438) and RMSE (10.91), significantly outperforming PID (IAE = 7.834, RMSE = 16.68) and conventional SMC (IAE = 4.257, RMSE = 12.42), indicating faster convergence and higher tracking accuracy. For the sinusoidal reference, FO-FSMC achieves the lowest IAE (1.534) and RMSE (2.286), showing slightly better performance than SMC (IAE = 1.585, RMSE = 3.086) and significantly outperforming PID (IAE = 1.955, RMSE = 3.983), demonstrating accurate tracking for smooth periodic inputs. For the pulse reference, the proposed FO-FSMC demonstrates substantial improvement over both PID and SMC, achieving the lowest IAE (6.58) and RMSE (16.05) compared to SMC (IAE = 9.32, RMSE = 19.77) and PID (IAE = 18.32, RMSE = 27.13), confirming faster convergence, higher tracking accuracy under abrupt changes. For the combined sinusoidal-step input, FO-FSMC achieves the lowest IAE (1.396) and RMSE (2.336), slightly better than SMC (IAE = 1.436, RMSE = 2.455) and clearly outperforming PID (IAE = 2.159, RMSE = 4.561), indicating precise and stable tracking even under hybrid continuous and abrupt reference variations. Thanks to the adaptive and intelligent tuning capabilities of fuzzy logic, the controller dynamically adjusts its gains in real time. Simultaneously, the sliding mode control ensures robustness and stability under nonlinear dynamics and time-varying conditions. Beyond that, the incorporation of fractional-order derivatives enables the controller to exploit the system's memory effects, leading to improved dynamic response, smoother control actions, and enhanced accuracy. This combined approach results in fast, accurate, and stable control, making FO-FSMC a highly effective choice for complex, nonlinear, and time-varying systems. Given that fuzzy logic is a core component

of intelligent control systems and fractional calculus has shown great promise in enhancing dynamic modeling and control accuracy, this work highlights how their integration can significantly improve the performance of real-world robotic systems. The proposed controller demonstrated faster response, higher tracking accuracy, and greater robustness, even despite the use of estimates in system dynamics in real-time implementation, confirming its effectiveness for controlling flexible robotic arms with enhanced accuracy and stability.

References

- [1] M. Uchiyama, A. Konno, T. Uchiyama, S. Kanda "Development of a flexible dual-arm manipulator testbed for space robotics", IEEE International Workshop on Intelligent Robots and Systems, Towards a New Frontier of Applications, vol.1, pp. 375-381, 1990, doi:10.1109/iros.1990.262413
- [2] H. Banerjee, Z. Tse, H. Ren, "Soft robotics with compliance and adaptation for biomedical applications and forthcoming challenges", International Journal of Robotics & Automation, Vol. 33, No. 1, 2018 doi:10.2316/journal.206.2018.1.206-4981
- [3] S. Mallikarjunaiah, S. Narayana Reddy, "Design of PID controller for flexible link manipulator", in: Proceedings of the 44th IEEE Conference on Decision and Control, Seville, Spain, 2005, pp. 6841-6846, doi:10.1109/CDC.2005.1583262
- [4] R. Fareh, M. Saad, "Adaptive control for a single flexible link manipulator using sliding mode technique", in: 6th International Multi-Conference on Systems, Signals and Devices, Djerba, Tunisia, 2009, pp. 1-6, doi:10.1109/SSD.2009.4956806
- [5] H.I. Abdulameer, M.J. Mohamed, "Fractional Order Fuzzy PID Controller Design for 2-Link Rigid Robot",

- International Journal of Intelligent Engineering and Systems, pp. 103-117, 2022, doi:10.22266/ijies2022.0630.10
- [6] H. Delavari, R. Ghaderi, N.A. Ranjbar, S.H. HosseinNia, S. Momani, "Adaptive fractional PID controller for robot manipulator", 4th IFAC Workshop On Fractional Differentiation And Its Applications, 2012, doi:10.48550/arXiv.1206.2027
- [7] H. Delavari, A. Azizkhani, P. Shiouoei, "Design and practical implementation of a fractional order PID controller for a single flexible-link robot", Tarbiat Modares University Journal System, vol. 17, No. 10, pp. 411-419, 2017 (in Persian), doi:10.1001.1.10275940.1396.17.10.28.6
- [8] F. Wang, P. Liu, F. Jing, B. Liu, W. Peng, M. Guo, M. Xie, "Sliding Mode Robust Active Disturbance Rejection Control for Single-Link Flexible Arm with Large Payload Variations", vol.10, pp. 2995, 2021, doi:10.3390/electronics10232995
- [9] H. Delavari, P. Lanusse, J. Sabatier, "Fractional order controller design for flexible link manipulator robot", Asian J Control, vol.15, No.3, pp. 783-795, doi:10.1002/asjc.677
- [10] A. Mujumdar, S. Kurode, B. Tamhane, "Fractional order sliding mode control for Single Link Flexible Manipulator", 2013 IEEE International Conference on Control Applications (CCA), Hyderabad, India, 2013, pp. 288-293, doi:10.1109/CCA.2013.6662773
- [11] R. Fareh, "Sliding Mode Fractional Order Control for a Single Flexible Link Manipulator", International Journal of Mechanical Engineering and Robotics Research, pp. 228-232, 2019, doi:10.18178/ijmerr.8.2.228-232
- [12] M. Raoufi, H. Delavari, "Experimental implementation of a novel model-free adaptive fractional order sliding mode controller for a flexible-link manipulator", International Journal of Adaptive Control and Signal Processing, Vol. 35, pp. 1990-2006, 2021, doi:10.1002/acs.3305
- [13] S. Ahmed, H. Wang, Y. Tian, "Adaptive fractional high-order terminal sliding mode control for nonlinear robotic manipulator under alternating loads", Asian Journal of Control, Vol. 23, pp. 1900-1910, 2020, doi:10.1002/asjc.2354
- [14] F. Hamzeh Nejad, A. Fayazi, H. Ghayoumi Zadeh, H. Fathi Marj, S.H. Hossein Nia, "Precise tip-positioning control of a single-link flexible arm using a fractional-order sliding mode controller", Journal of Vibration and Control, vol. 28, pp. 1683-1696, 2020, doi:10.1177/1077546320902548
- [15] Kh. B. Gaufan, M. Badamasi Aremu, Nezar M. Alyazidi, A. Nasir, "Robust fractional-order sliding mode control for robotic manipulator system with time-varying disturbances", Franklin Open, Vol. 12, September 2025, 100287, https://doi.org/10.1016/j.fraope.2025.100287
- [16] O.C. Ozguney, R. Burkan, "Fuzzy-Terminal Sliding Mode Control of a Flexible Link Manipulator", Acta Polytechnica Hungarica, Vol. 18, No. 3, pp. 179-195, 2021, doi:10.12700/APH.18.3.2021.3.10
- [17] B.A. Bazzi N.G. Chalhoub, "Fuzzy Sliding Mode Controller for a Flexible Single-Link Robotic Manipulator", Journal of Vibration and Control, Vol. 11, pp. 295-314, 2005, doi:10.1177/1077546305049480
- [18] M.H. Korayem, S.F. Dehkordi, O. Mehrjooee, "Nonlinear analysis of open-chain flexible manipulator with time-dependent structure", Advances in Space Research, Volume 69, Issue 2, pp. 1027-1049, 2022, https://doi.org/10.1016/j.asr.2021.10.037
- [19] N. Yousefi Lademakhi, P. Moradi, M. H. Korayem, "Experimental identification of dynamic friction parameters with the intention of precision optimal control of model based robotic systems", 2022 8th International Conference on Control, Instrumentation and Automation (ICCIA), 10.1109/ICCIA54998.2022.9737173
- [20] H. Zohoor, F. Kakavand, "Timoshenko versus Euler–Bernoulli beam theories for high speed two-link manipulator", Scientia Iranica, Vol. 20, pp. 172-178, 2013, https://doi.org/10.1016/j.scient.2012.12.016
- [21] ROBOTIS e-Manual v1.25.00, Instruction Packet, 2010; http://www.support.robotica.com/en/product/dynamixel/communication/dxl_pac/.
- [22] ROBOTIS e-Manual v1.25.00, Kind of Instruction, 2010; http://www.support.robotica.com/en/product/dynamixel/communication/dxl_ins/.
- [23] ROBOTIS e-Manual v1.25.00, Data Sheet, 2010; http://www.support.robotica.com/en/product/dynamixel/communication/.
- [24] M.R. Faieghi, H. Delavari, D. Baleanu, "Control of an uncertain fractional-order Liu system via fuzzy fractional-order sliding mode control", Journal of Vibration and Control, Vol. 18, pp. 1366-1374, 2011, doi:10.1177/1077546311422243
- [25] H. Delavari, R. Ghaderi, A. Ranjbar, S. Momani, "Fuzzy fractional order sliding mode controller for nonlinear systems", Communications in Nonlinear Science and Numerical Simulation, vol. 15, pp. 963-978, 2010, doi:10.1016/j.cnsns.2009.05.025
- [26] H. Delavari, H. Heydari Nejad, "Applied fractional order nonlinear control", Hamedan: Hamedan University of Technology Press, 2019 (in Persian)